Particle-level phenomena and macroscale soil behavior

J. C. Santamarina
Georgia Institute of Technology, Atlanta, Georgia, USA

ABSTRACT: Soils are particulate materials; fluids and microorganisms fill the pore space. Salient particle level phenomena include fluid-mineral interaction, mixed fluid phase interaction, bio-mediated geochemical processes, size-dependent particle level forces, particle-shape effects, columnar force transfer along the granular skeleton, and multiple internal temporal and spatial scales. These phenomena manifest into complex macro-scale soil response including inherent non-linear and non-elastic behavior; stress-dependent stiffness, strength and volume change; porous and pervious material, inherent and stress-induced anisotropy, time-dependent response, and energy coupling among others. Selected particle-level processes and macroscale behaviors are reviewed.

1 INTRODUCTION

The empirical understanding of soil behavior evolved long before its fundamental understanding. The concept of effective stress has its roots in Archimedes (II BC), and it is elaborated in soils and porous media by Terzaghi and Biot (1920's-1930's). Egyptians (XXVII BC) knew how to control friction, which is later analyzed by daVinci (XVI) and Coulomb (XVIII). Reynolds demonstrated dilatancy (XIX); the interplay between shear stress, volume and confining stress is developed by Taylor, Roscoe, and Schofield (1940's-1960's). Suction induced shrinkage was known to the Babylonians (XXIII BC), yet the comprehensive understanding of partial saturation takes place in the 1960's with contributions by Aitchison, Bishop, Morgenstern and Fredlund. The theoretical framework for seepage was advanced by Laplace, the Bernoulli's and Darcy (XVIII-XIX). Long recognized plasticity is investigated by Goldschmidt in the 1920's and Lambe and Mitchell in the 1950's, after colloidal theory is advanced by Guy, Chapman, Stern, Debye and Huckel in the period from 1910 to 1930. The inherent non-linear and non-elastic behavior of soils is explained at the particle level by Hertz (1870's) and Mindlin (1950's) contact theories.

Today, new tools and technological developments open unprecedented possibilities to understand soil behavior and to engineer its response. Such technological advances include discrete element modeling, molecular dynamics, atomic force microscopy, and a wide range of high resolution non destructive techniques and tomographers (e.g., micro-tomographers, magnetic resonance imaging).

The purpose of this manuscript is to present a concise analysis of salient particle-level phenomena and processes in order to comprehend the macroscale soil response. Soil components are analyzed first leading to soil packing and fabric formation. Then, selected macroscale responses are discussed.

2 SOIL COMPONENTS

Soils are particulate materials. Mineral particles form the granular skeleton and the interparticle porosity is filled with one or more fluids. The pore space may also include microorganisms (Figure 1).

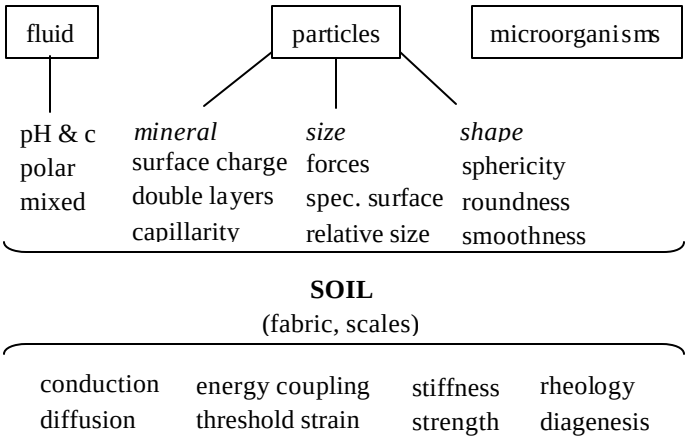

Figure 1. Soils. Particle-level properties and macro-response.

2.1 *Pore fluid*

The fluid that fills the pores left by the mineral particles is either a single-phase fluid, typically water in saturated soils, or a mixed-phase fluid, such as water and air (typical in partially saturated soils), or water and an immiscible organic fluid (e.g., contaminated soils or petroleum reservoirs).

When water is the prevailing fluid, the ionic concentration and the pH determine -and reflect- the interaction between the mineral and the water (Figure 2-a). Typically, the pore fluid in soils is an aqueous electrolyte consisting of free water molecules and hydrated ions. The water molecule polarity aided by thermal vibration makes water an effective solvent. Water can dissolve salt until it reaches the "saturation concentration", which for NaCl is 350 g/lt near freezing and 390 g/lt near boiling. For comparison, the ionic concentration is 0.001 g/lt for fresh water, and about 35 g/lt for seawater.

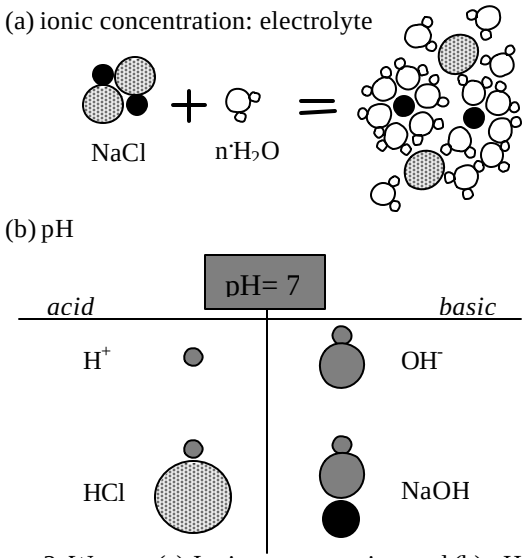

Figure 2. Water - (a) Ionic concentration and (b) pH.

The value of pH is a measure of the relative balance between hydrogens and hydroxyls in the water-base solution. The pH=7 when the number of hydrogens and hydroxyls is balanced. However, if a substance such as chloric acid is added, the number of hydrogens exceeds that of hydroxyls and pH<7 (Figure 2-b). Alternatively, hydroxyls may be incorporated, for example by adding sodium hydroxide, and the water pH increases, pH>7. The relevance of ionic concentration and pH will become apparent when minerals are taken into consideration.

Molecules at the interface between two immiscible fluids are not randomly oriented because of the different interaction forces they experience to each fluid. This molecular-level effect results in a contractile, membrane-like interface at the macroscale. The "surface tension" in this membrane depends on the properties of the two interactive fluids. Figure 3-a shows the formation of a capillary meniscus at the interface between two spherical particles.

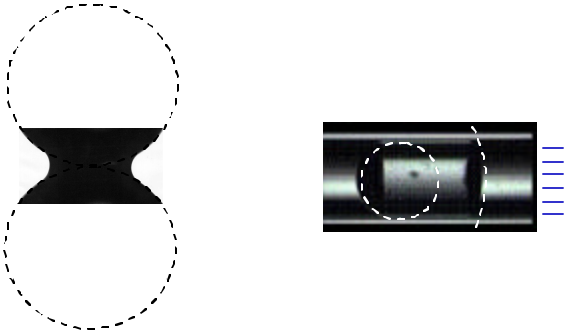

Figure 3. Mixed fluids. Microphotographs: (a) Meniscus between two 1mm diameter glass beads. (b) Water drop in 1mm capillary tube subjected to differential pressure (Alvarellos 2003) - Note that the contact angle is not constant when there are interacting menisci.

The angle formed between the fluid interface and the mineral surface is called the contact angle. The shallower the contact angle, the more "wetting" the fluid is. Soils surrounded by oil may become "oil-wet", even though most minerals tend to prefer water-wet conditions due to the mineral structure itself. In general, the contact angle is assumed constant for a given fluid-substrate system. However, menisci that form between different particles interact through the fluid pressure, and the resulting contact angles are not the same (Figure 3-b). Given these complexities, the analysis and scaling of microscale effects in partially saturated particulate media is complex.

2.2 *Particles*

2.2.1 *Mineralogy*

Each soil grain is typically made of a single mineral, except in some coarse sands and gravels. The mineralogy in coarse grains determines the grain stiffness, strength, hardness, abrasiveness and crushability. For example, the crushing yield stress is >10MPa for quartz sand and <0.2 MPa for carbonate sands.

The role of mineralogy in fine-grained soils is more subtle, yet more important. Clay minerals are made of layers of silicates and aluminates, and are known as phyllosilicates. Figure 4 shows the chemical structure of kaolinite and montmorillonite. The analysis of these sketches reveals the presence of either oxygen or hydroxyls on the surface of clay minerals, thus the affinity of clay surfaces to either the hydrogens or hydroxyls in water. It also hints to the importance of pH: indeed, the dissolution or precipitation of clay minerals and the surface charge will be controlled by the pH of the pore fluid.

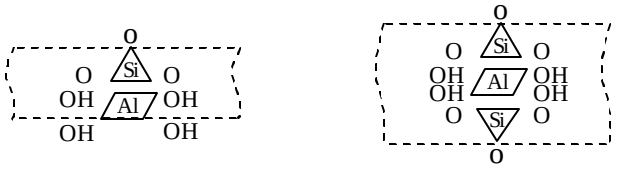

Figure 4. Clay minerals - single sheet. Notice differences among the surfaces. (a) Kaolinite - a particle is made of many similar sheets. (b) Montmorillonite (see Velde 1992)

If the clay surface exhibits charge, then there will be counterions in the vicinity of the clay mineral to ensure electro neutrality. Counterions do not bond onto the clay surface in the presence of water because of the thermal agitation of water molecules that continue hydrating and colliding with these ions; instead, counterions remain in the vicinity of the clay surface forming a counterion cloud. The higher the ionic concentration in the pore fluid, the thinner the cloud becomes.

In summary, the pore fluid pH and ionic concentration affect surface charge and the thickness of the counterion cloud near mineral surfaces.

2.2.2 *Size (particle-level forces)*

Particle-level forces are linear, quadratic or cubic functions of the particle size d (Table 1). Simple force-equilibrium analyses between these forces show that: (1) particles larger than 10-to-100 microns are controlled by the interparticle skeletal forces that result from the applied effective stress; while (2) both capillary and electrical forces prevail for smaller particles.

Table 1. Particle-level forces - Note particle-size dependency.

Skeletal	$N = \sigma' d^2$
Weight	$W = (\pi G_s \gamma_w / 6) d^3$
Buoyant	$U = (\pi \gamma_w / 6) d^3$
Hydrodyn.	$F_{drag} = 3\pi\mu v d$
Capillary	$F_{cap} = \pi T_s d$
El. attraction	$Att = A_h d / 24 t^2$
El. repulsion	$Rep = 0.0024 \sqrt{c_o}\ e^{-10^8 t\sqrt{c_o}}\ d$
Cementation	$T = \pi \sigma_{ten} t d$

The drastic change in governing physical forces and related processes among fine and coarse grained soils is recognized by the Unified Soil Classification System USCS, and its emphasis on sieve #200 (76μm). In the case of coarse soils with no fines, the USCS also requires the determination of the coefficient of uniformity $C_u=D_{60}/D_{10}$: when particles of different size are present, the smaller particles fit between the voids left by the larger particles and soils exhibit lower terminal void ratios e_{max}, e_{min} and those on the critical state line.

Smaller particles that are not part of the load-carrying granular skeleton can be dragged by seeping fluids, and migrate. A small particle d_{small} will be retained at the pore throat formed by larger particles d_{large} when it is larger than the size of the pore throat $d_{small}=d_{throat}$, which is about d_{throat}~0.2-to-0.4d_{large} (Figure 5-a). When many small particles migrate, they may reach the pore throat and form a bridge (Figure 5-b). Particle-level experimental results by Valdes (2002) show that migrating particles can be retained by bridge formation when they are about $d_{small}>0.2d_{throat}$, therefore d_{small}~d_{large}/(10-to-25). These observations are the particle-level justification of empirically developed filter criteria (Terzaghi et al., 1996).

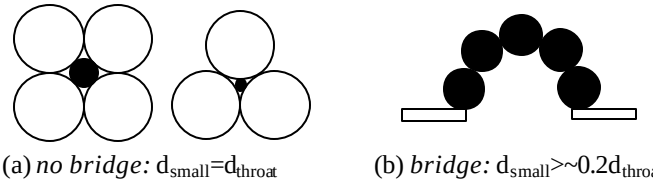

(a) *no bridge:* $d_{small}=d_{throat}$ (b) *bridge:* d_{small}>~0.2d_{throat}

Figure 5. Fines migration and filter criteria at the particle level. (a) Single migrating particle passing condition. (b) Bridge formation in multiple migrating particles.

2.2.3 *Specific surface*

Surface related phenomena, such as chemical reactions and viscous drag in seepage are not determined by particle size per se, but by surface area. The specific surface S_s is defined as the ratio between the surface area and the mass of the particle. When a $1m^3$ cube is split into smaller pieces, the total mass of the cube remains constant, however the surface area increases dramatically. In other words, the specific surface increases as the particle size decreases.

Specific surface reflects both particle size and shape. Spherical particles exhibit the least amount of surface for a given volume; however, when a spherical particle is flattened, it develops a surface that is inversely proportional to the thickness of the flattened particle. In general, the specific surface is determined by the smallest dimension of the particle L_{min}, e.g., the thickness of platy particles or the diameter of cylindrical particles. The theoretical maximum value a particle can reach before it looses its mineralogical identity is estimated to be ~$2000m^2/g$. The specific surface can range from more than a 1000 m^2/g for amorphous silica to less than $10^{-4}m^2/g$ for coarse sands as shown in Figure 6.

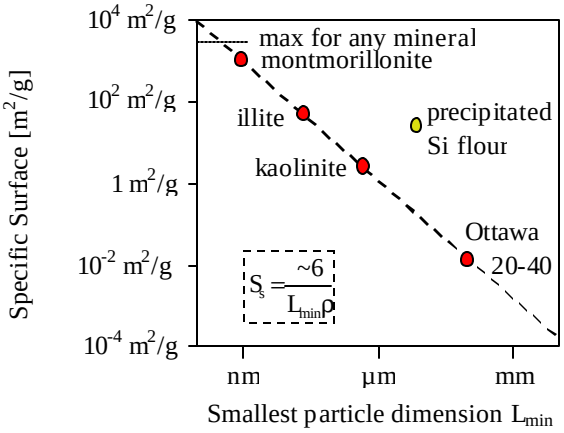

Figure 6 Specific surface and particle size (? is the mineral mass density). Precipitated silica flour deviates from the general S_s-vs-L_{min} trend observed for uniform soils; electron microphotographs show that the uniform silt-size particles are made of submicron particles.

Sieve analysis permits identifying the various fractions in a soil. The resulting distribution is based on mass. Grain size distribution can also be explored in terms of the contribution each fraction makes to the total specific surface of the soil. Figure 7 shows (a) grain size distribution in terms of "cumulative mass", (b) the corresponding density function, i.e., the percentage of each fraction, (c) the density function in terms of surface contributed by each fraction, and (d) the cumulative grain size distribution in terms of surface area. The surface-based distribution is always shifted towards the finer sizes due to their higher contribution to total surface. The surface-based grain size distribution is a more meaningful representation of the soil for surface-dependent processes, such as seepage, diffusion retardation, chemo-mechanical coupling, and geochemistry in general.

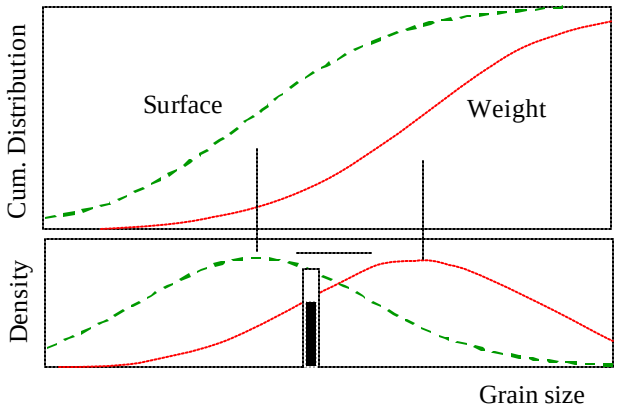

Figure 7 Mass-based and surface-based grain size distributions.

2.2.4 *Shape*

The emphasis on particle size and relative size in that Unified Soil Classification System conceals the importance of particle shape on soil behavior. Particle shape has three different scales: global shape (sphericity, platiness); bumps and corners (roundness, angularity); and small surface perturbations (smoothness, roughness), as shown in Figure 8.

The shape of particles larger than ~50µm is determined by mechanical action such as fractures, dislocations and collisions. However, the shape of particles finer than ~50 µm is controlled by chemical reactions.

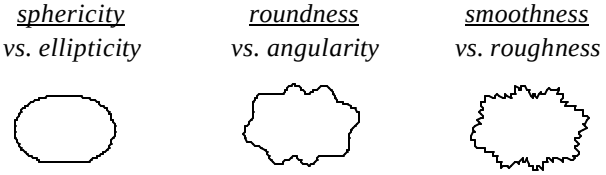

Figure 8. Scales in particle shape. Examples of deviations from sphericity: precipitated carbonate; from roundness: crushed sand; from smoothness: forminiferan.

2.3 *Microorganisms*

The role of microorganisms in soils has been recognized and extensively studied in agriculture and in geoenvironmental remediation, but overlooked in geomechanics.

The size of bacteria is in the order of 1μm (spores can be as small as 0.2μm), therefore, there could be ~10^8 bacteria/mm^3 of pore space. Given the high reproduction rate (duplication every 20-to-60 minutes), microbial activity rapidly adapts to the most diverse environments, from very cold to very hot, from acidic to basic. Hence, there is exceptional bio diversity and ubiquitous presence of microorganisms.

Life requires (1) nutrients, i.e., energy source and carbon for cell mass, (2) water, and (3) proper environmental conditions such as pH, salinity, temperature, and sufficient space. Any of these components can become the limiting factor and restrict life in soils. From this point of view, bacterial activity is space-limited in clayey soils.

While the biological effects on geomechanical behavior are still underexplored, promising areas for further investigation include bio-mediated geochemical reactions and short-term cementation/digenesis, clogging and changes in hydraulic conductivity, and gas generation.

3 PACKING AND FABRIC

Governing forces lead to different fabric formation mechanisms in coarse particles (d>50-to-100μm) and in fine particles (d<10-to-50 μm).

The packing of coarse grain soils is determined by particle shape and the relative size of the particles. Shape affects particle mobility and their ability to attain the minimum energy configuration; hence, non-spherical, angular or rough particles pack in looser states. As discussed earlier, relative size determines the ability of small particles to fit in the voids left by larger particles. Expressions for e_{max} and e_{min} as a function of roundness R for C_u=1 follow (Youd, 1973):

$$e_{max} = 0.554 + 0.154\ R^{-1} \quad (1)$$

$$e_{min} = 0.359 + 0.082\ R^{-1} \quad (2)$$

Non spherical particles tend to sediment with their longest axis on the horizontal plane (minimum potential energy), causing inherent fabric anisotropy. Platy mica particles bridge over voids left by rounded particles beneath it, and enforce the alignment of rounded particles above the sheet. The combination of ordering and bridging makes the void ratio of the soil a function of the percentage of mica and the relative size of mica with respect to the size of round particles (Guimaraes, 2002).

In fine particles, pH and ionic concentration determine fabric formation. At low ionic concentration, edge-to-face aggregation takes place at intermediate pH values, and dispersed structures at either high or low pH. On the other hand, when the ionic concentration is high, the counterion cloud shrinks, the osmotic repulsion decreases and van der Waals attraction prevails causing face-to-face aggregation. A schematic fabric map is presented in Figure 9 (extensive experimental evidence can be found in Palomino 2003). The transition pH and ionic concentration depend on the type of clay mineral as well as the type of ions present in the pore fluid.

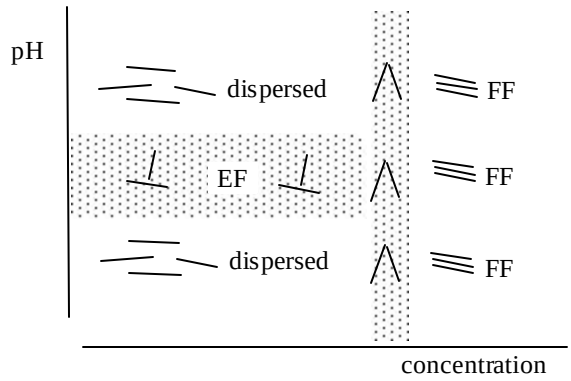

Figure 9. Schematic fabric map applicable to fine-grained soils (controlled by electrical forces). Ionic concentration and pH values in transition zones are mineral specific. EF flocculation may not take place in very thin montmorillonite particles.

4 MACROSCALE SOIL BEHAVIOR

The macroscale response of a soil mass reflects underlying microscale processes that are associated with mechanisms and variables described in the previous sections. In this section, selected macroscale behaviors are analyzed at the microscale, including the mechanical response at small and large-strain, time dependent phenomena, and multiple internal scales.

4.1 *Strain-dependent mechanical response*

The mechanical behavior of the soil skeleton is strain-dependent, and very different microscale

mechanisms develop when small-strain-constant-fabric and large-strain-fabric-changing excitations are imposed.

4.1.1 *Small-strain*

The mechanical response at small strains takes place at constant fabric, and the deformation concentrates at contacts, the stiffness is maximal, energy losses and volume changes are minimal, and diagenetic effects exert the highest influence.

Deformation at constant fabric means that particles do not lose or change neighboring particles. Therefore, the small strain stiffness (and Poisson's ratio) of the soil reflects contact deformation. In the case of coarse grains, contact stiffness is determined by the deformability of the particle and asperities near the contact (theoretical analog: Hertzian contact). In the case of fine grains the intuitive concept of solid-to-solid contact losses relevance, and interparticle interaction takes place through interparticle electrical forces.

The small-strain shear stiffness for both fine and coarse soils is a power-function of the effective confining stress. In terms of the shear wave velocity V_s,

$$V_s = \alpha \left(\frac{\sigma'_{\text{propagation}} + \sigma'_{\text{particle motion}}}{2\,\text{kPa}} \right)^{\beta} \qquad (3)$$

where the parameters a and ß are experimentally determined. Extensive experimental evidence shows that a and ß are inherently interrelated as:

$$\beta = 0.36 - \alpha / 700 \qquad \text{where a [m/s]} \qquad (4)$$

The value of the exponent is ß=0.17-0.20 for dense, rounded sands and can exceed ß=0.3 for soft clays. The value of ß increases for loose sands, soft clays, angular and/or rough grains, and soils with mica. On the other hand, ß? 0 for overconsolidated clays and cemented sands before yield. As the degree of cementation increases, the localized deformation at contacts decreases, the soil stiffness increases, the stress sensitivity of the soil stiffness decreases (lower ß), and the stress that is required to regain the stress-dependence stiffness of the soil mass increases.

Partial saturation adds capillary forces between particles beyond those carried by the applied effective stress. Therefore, a drying soil will exhibit increasing stiffness unless massive shrinkage fractures develop.

Small-strain anisotropy reflects inherent fabric anisotropy. Post depositional changes due to loading or cementation affect the degree of anisotropy.

4.1.2 *Large-strain*

The large-strain mechanical response involves fabric change, and contact deformation plays a diminishing effect. Stiffness decreases with increasing strain, and important energy losses take place - mostly of frictional nature.

The increase in mean effective stress causes volume contraction. However, either contraction or dilation results from applied deviatoric stresses as a result of two competing microscale effects: dilation to overcome rotational frustration in particles with high coordination, and chain buckling and collapse when particles have low coordination. At very large strains, the balance between local collapse and local dilation reaches statistical equilibrium, the soil shears at a constant volume f_{cv}, and the soil fabric approaches the "critical state fabric".

The friction angle of the soil when shearing at constant volume is determined by particle shape, including sphericity, roundness, and roughness. In terms of roundness R (Santamarina & Cho 2004),

$$\varphi_{cv} = 42 - 17R \qquad (5)$$

The constant volume friction angle in sands has been correlated with the angle of repose. However, the angle of repose is different when it is measured for a sand cone f_{ext}, a planar surface, or an inside flow cone f_{int} (e.g., when a central plug beneath a filled cylinder is removed). Data presented in Figure 10 show that the internal angle of repose f_{int} is significantly greater than the external angle f_{ext}. The internal flow experiences a gradual reduction in cross section (~2D flow gradually becomes 1D as in lateral compression LC), while flow on the external slope experiences a gradual increase in cross section (as in lateral extension LE). At the microscale, interparticle coordination in the annular direction increases in the first case (f_{int}) while it decreases in the second case (f_{ext}). Similar friction angle anisotropy is observed in triaxial axial extension AE and axial compression cases AC, both sands and clays (Mayne and Holtz 1985).

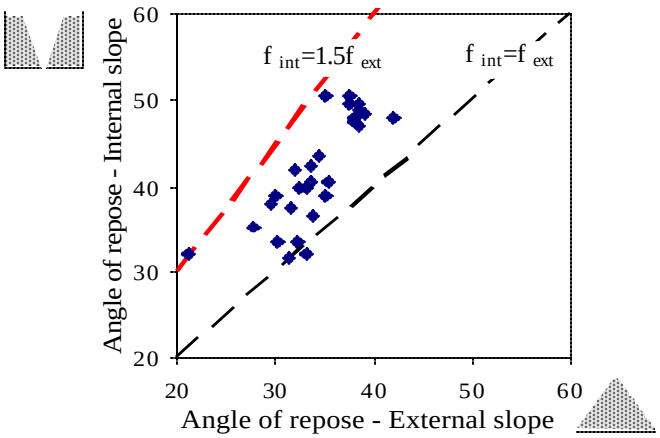

Figure 10. Friction anisotropy (several studies with natural and crushed sands - compiled by G. Narsilio).

The undrained shear strength also exhibits anisotropy. However, in this case, anisotropy is controlled by pore pressure generation following skeletal collapse upon loading. In general, the particle chains that carry load tend to be more stable for continuous loading in the same direction than for sudden transverse loading. Therefore, the undrained shear strength in axial extension is lower than in axial compression (Ladd et al. 1977; Mayne & Holtz, 1985; Zdravkovic & Jardine 1997; Yoshimine et al. 1999).

Particle shape determines the very large-strain residual shear strength where the higher the platiness of particles, the lower the residual friction angle. Non-spherical particles tend to develop anisotropic fabrics. The compressibility of anisotropic fabrics in the vertical and the horizontal directions are quite distinct. These will affect the generation of pore pressure during undrained loading. Therefore, the shear strength of anisotropic fabrics can be dramatically different for dissimilar loading paths (Leroueil & Hight 2003).

4.1.3 *Elastic threshold strain*

The transition from small to large-strain behavior is not abrupt but gradual. The beginning of modulus degradation denotes the "linear threshold strain" $?_{dt}$, which depends on the nature of particle-to-particle interactions (Figure 11). For mechanical Hertzian contacts, the amount a particle can deform before detaching depends on the mineral stiffness G_s and the initial flatness of the contact due to the applied initial confining stress s'. For interparticle interaction of electrical nature, the separation between two particles before ending interaction is related to the thickness of the counterion cloud ?. Then, the threshold strain is proportional to the ratio between the thickness of the adsorbed layer and the particle size. This ratio also affects soil plasticity, therefore, the linear threshold strain in clayey soils is correlated with the plasticity of the soil (details and discussion in Santamarina et al., 2001; Experimental evidence in Vucetic & Dobry 1991).

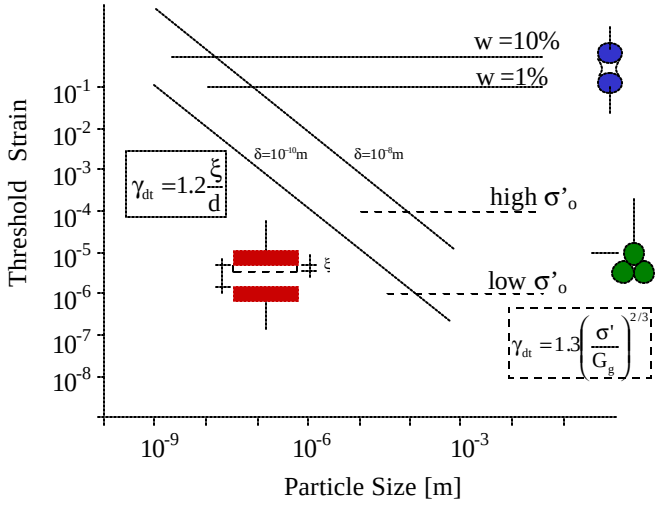

Figure 11. Particle-level estimation of elastic threshold strain for different contact mechanisms.

4.2 *Short Term Effects - Rheology*

Time-dependent changes highlight non-equilibrium conditions after the application of load, including gradients of chemical, electrical, mechanical or thermal origin. Macroscale boundary criteria (such as isothermal, constant composition, and constant volume) do not apply at the microscale, and local thermal, chemical, mechanical or electrical transport can take place.

A stable soil under constant boundary conditions is at the bottom of an energy well, and any change will require overcoming some energy threshold (frictional threshold at each contact or energy well for ions in Stern layer). A perturbation may contribute to overcoming the corresponding energy barriers, triggering internal changes. Once the process is initiated, internally liberated energy, for example in the form of acoustic emission, may continue to sustain the process of change until a new global energy well is reached.

More recently, the relevance of strain rate on mechanical soil properties is gaining increased atten-

tion. Related macroscale behavior include (Tatsuoka et al. 2003):

- "isotach response" where the strength and stiffness increase when the strain rate increases, such as in low plasticity Pleistocene clays and soft rocks; and
- "viscous evanescence" where the same stress-strain behavior is observed at all strain rates however a transient is measured when the strain rate changes, such as in sands.

Such behavior can have important engineering implications. For example, if the undrained strength increases at a rate of 10% per log cycle of strain rate (Kulhawy & Mayne 1990), then how should in situ and standard laboratory tests (? ~1-10^{-2}/min) be analyzed to provide strength data relevant to foundation construction ?~10^{-7}-10^{-8}/min (Randolph 2002)?

Several microscale mechanisms are hypothesized next as potential contributors to short term rheological effects. Soil testing to identify the prevailing mechanism requires procedures that vary strain rate, temperature (activation energy), and pore fluid (dry air, and fluids of different permittivity).

4.2.1 *Contact-level mineral creep and friction*

Mineral creep and interparticle friction are complex phenomena, which are exacerbated by interparticle interactions throughout the granular skeleton. Salient comments follow.

- Mineral creep at contacts. Numerical micromechanical simulations (Kuhn & Mitchell, 1993; Rothenburg 1992) and photoelastic model studies (Díaz-Rodríguez & Santamarina 1999) show that contact creep cause: force redistribution, changes in load-carrying granular chains, increase the global coordination number, and significant increase in small strain stiffness (Cascante & Santamarina, 1996). In fact, the higher the variability in contact forces the higher the global creep rate.
- The velocity dependency of friction is affected by the presence of water and the development of boundary and hydrodynamic lubrication. Furthermore, a frictional transient is observed upon changes in velocity - similar to macroscale viscous evanescence (Figure 12 - Dieterich 1978)
- Non-linear coupling between friction and noise (noise may be generated by a nearby slippage). Low amplitude vibrations can accelerate thixotropic effects in soils; this is known as rheopexy in clays and cyclic pre-straining in sands.

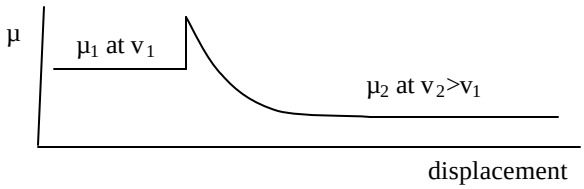

Figure 12. Transient in mineral-to-mineral frictional response when velocity v is increased from v_1 to $v_2>v_1$.

4.2.2 *Fluid migration*

Mechanisms related to pore fluid migration apply to both saturated and partially saturated soils:

- Mitchell (1960) measured the rate of thixotropic regain at different temperatures and estimated the activation energy of the process to be 3-4 kcal/mol, which suggests that viscous flow of water as the underlying mechanism.
- Moisture migration in partially saturated soils, is relatively fast - via conduction- in high saturation cases, yet it is slow in low saturation conditions as it takes place through and through the vapor pressure

4.2.3 *Surface chemistry and phenomena*

The role of adsorbed layers on time-dependent processes has long been recognized, for example, thixotropic behavior is often related to flocculation prone clay systems (see Van Olphen, 1951, Mitchell, 1960). Mechanisms under this category relate to

- Ion diffusion in adsorbed layers following disturbance by inter-contact relative displacement
- Atomic stick-slip in adsorbed layers (Landman et al. 1996; Persson 1998)
- Pressure solution-precipitation
- Cementation (may be bio-mediated)

4.2.4 *Time*

Time-dependency implies underlying inertial, conduction (includes viscous) or diffusional processes. Simple scale analyses permit estimating the mean time scales:

$$t_{displace} = \frac{\varepsilon}{\dot{\varepsilon}} \qquad \text{imposed} \qquad (6)$$

$$t_{inertia} = d\sqrt{\frac{\rho}{\sigma'}} \qquad \text{particle-inertial} \qquad (7)$$

$$t_{conduct} = \frac{d}{ki} \qquad \text{local conduction} \qquad (8)$$

$$t_{diffuse} = \frac{\varepsilon^2 d^2}{D} \qquad \text{local diffusion} \qquad (9)$$

where e= strain, ?= strain rate, k= conductivity, i= gradient, and D=diffusion coefficient.

Evidence for very high local hydraulic gradients i is available in other poroelastic media such as bones, (Wang et al 2003). The time for local diffusion (Equation 9) is required for counterion reorganization after an imposed disturbance equal to ed. Interparticle repulsion continues changing during this time.

Time dependent effects should be expected when the local, particle level processes cannot keep up with the rate of disturbance. For example, when, $t_{displace} << t_{diffuse}$, the expected strain rate is $?>>D/ed^2$. The diffusion coefficient for ions in the adsorbed layer varies between $D \sim 10^{-10} m^2 s^{-1}$ to the bulk $D \sim 10^{-9} m^2 s^{-1}$. Therefore, for a strain $e=10^{-2}$, and particle size $d=10^{-3}$m, the predicted strain rate for this phenomenon is $?>10^{-2} s^{-1}$.

"Domino" effects throughout the granular skeleton extend the effective duration of contact-level phenomena (Figure 13 - experimental evidence: duration of acoustic emission after a transient excitation). In some respects, the phenomenon resembles queuing: the expected wait in a queue if customers arrive at a certain rate 'c' and are served at rate 's', where both events have some known distribution, e.g., Poisson. If applicable, the mathematics of queuing theory can be invoked to further analyze the effective macroscale time of the process.

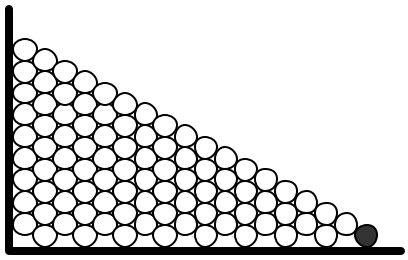

Figure 13. Duration of macroscale processes. If the black marble is suddenly displaced outwards a distance d, how long will the marble at the top of the pile experience displacement?

4.3 *Variability and scales*

The topic of scales must take into consideration spatial and temporal scales corresponding to the soil mass and the imposed excitations, identification of emergent phenomena (e.g., water gap formation in heterogeneous media subjected to dynamic loading - Fiegel & Kutter 1994; Kokusho 1999), effective properties for design and related engineering implications.

The soil mass and the soil response exhibit very characteristic temporal and spatial scales. Spatial scales L can be identified from the particle level (e.g., roughness and particle size), at intermediate scales (e.g., aggregations and spatial variability in void ratio), and at the level of the engineering system (e.g., layers and macro-heterogeneity). Temporal scales for conduction $t_{cond} \sim L/ki$, diffusion $t_{dif} \sim L^2/D$, and vibration $t_{vib}=2pv(m/k^*) \sim 2pL/V_s$ (k^*: stiffness; m: mass; V_s: shear wave velocity) are related to the spatial scale L of the soil mass and/or system, and the corresponding material parameter (similar to Equations 7, 8 and 9). The associated times can range from 0.1μs for chemical diffusion across the double layers, to years for pressure diffusion consolidation in thick soil layers.

The temporal and spatial scales of the imposed excitation (mechanical, thermal, chemical, electrical or biological) vary from ms to quasi-static, and from cm to regional (Table 2).

Table 2. Spatial and temporal scales in the excitation

Excitation	Spatial [m]	Time [s]
In situ testing	10^{-2}	1
Truck at 100 km/hr	10^{-1}	10^{-2}
Seismic excitation	10^{0}-region (a)	10^{-1}-10^{2} (b)
Building construction	10^{1} m	10^{7}
Landfill	10^{2} m	quasi-static

Notes: (a) spatial scale varies with system under consideration; (b) there are two temporal scales: one related to frequency content and the other to the duration of the event.

The comparison between the internal scales and the scale of the imposed excitation determines the nature of the excitation-soil interaction. In terms of time scales, drained loading applies when the time for load application t_{load} is greater than the time for pressure dissipation ($t_{load} > t_{dif}$), quasi-static analyses apply when $t_{load} >> t_{vib}$, remediation is diffusion-control when $t_{cond} < t_{dif}$.

In terms of spatial scales, the comparison between the scale of the medium and the excitation affect the choice of analysis, for example, block theory should be used when the scale of the structure (e.g., tunnel diameter) is similar to the joint spacing, otherwise equivalent continuum models apply.

In a spatially varying soil mass, the effective properties for design depend on (1) the value of the selected material property for each component k_i present in the region affected by the excitation, (2) the volumetric or gravimetric fraction of each com-

ponent f_i, and (3) their spatial distribution. Consider proportional properties k between input and output, such as conductivity [gradient? flow rate] and compliance [force? deformation] rather than stiffness. The equivalent "effective" value k_{eq} can be empirically fitted with a power average law:

$$k_{eq} = \left[\sum_i f_i (k_i)^{\alpha} \right]^{\frac{1}{\alpha}} \qquad f_i<1, \ ? \ f_i=1.0, \ 1=a=-1 \qquad (10)$$

where k_i is the value of the property for the i^{th} component and f_i its volumetric or gravimetric fraction. The exponent a is related to the spatial arrangement of the components and the physical nature of their interaction. Special cases of the power average expression are listed next for a medium made of two materials:

$$k_{eq} = f_1 k_1 + (1-f_1) k_2 \qquad a=1 \qquad \textit{parallel} \qquad (11)$$

$$k_{eq} = \left[f_1 \sqrt{k_1} + (1-f_1) \sqrt{k_2} \right]^2 \qquad a=1/2 \qquad \textit{CRIM} \qquad (12)$$

$$k_{eq} = k_1 \left(\frac{k_2}{k_1} \right)^{(1-f_1)} \qquad a=0 \qquad (13)$$

$$k_{eq} = \left[\frac{f_1}{k_1} + \frac{(1-f_1)}{k_2} \right]^{-1} \qquad a=-1 \qquad \textit{series} \qquad (14)$$

Figure 14 shows the predicted trends, and highlights the importance that spatial distribution has on the effective property of the medium. For example, for $f_1=0.9$ and $k_2/k_1=10$, the effective property of the medium would be $k_{eq}=1.9k_1$ when components are in parallel and $k_{eq}=1.1k_1$ if components are in series. Upper and lower bounds can be estimated for different phenomena in the absence of spatial distribution information (e.g., Hashin-Shtrikman bounds for stiffness and conduction can be found in Mavko et al. 1998).

5 CLOSING THOUGHTS

Soils are particulate materials, therefore, soils are inherently non-linear and non-elastic; strength, stiffness, and volume change are effective stress dependent; and they are inherently porous and pervious.

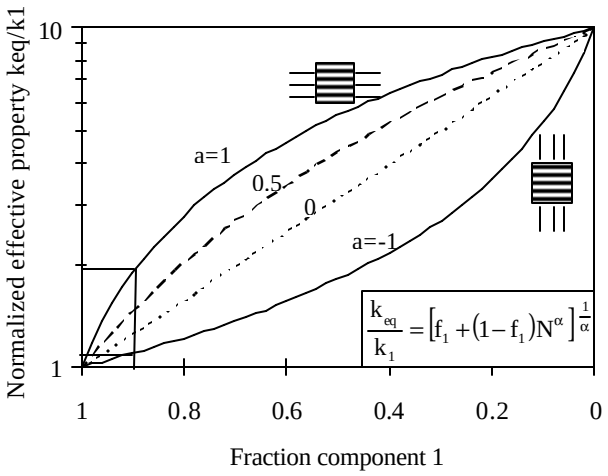

Figure 14. Effective media properties. Power average law.

The unified soil classification makes a critical distinction between coarse and fine soils. The choice of the Sieve #200 is compatible with the transition in governing interparticle forces and the balance between mechanical and chemical processes within the soil mass. Micromechanical analyses also support the use of C_u for coarse soils and the plasticity chart for fine soils. Additional "index properties" would enhance soil classification, including: (1) specific surface, ph and ionic concentration in clayey soils, and (2) particle shape in sandy and gravely soils.

Macroscale phenomena (such as deformation, strength and strength anisotropy, conduction and clogging), are functions of distinct micro-scale processes. Fundamentally different particle-level mechanisms participate in small and large strain soil deformation. Time scales observed at the macroscale (e.g., strain rate effects) can be significantly different from those observed at the particle-level.

Engineering design is affected by internal temporal and spatial scales. Effective properties for design depend on the properties of the participating materials, their fractions, and their spatial distribution. Enhanced detection and site characterization are needed to properly consider spatial variability.

There is great bio-diversity in the subsurface. Therefore there are unique opportunities to harness this potential. Due to space-limiting conditions, silty and sandy soils are preferred to explore biogeochemical processes control.

Today's particle level understanding of soil behavior, complemented with new testing and instrumentation technology open unique opportunities to

unprecedented developments in engineering soil behavior.

ACKNOWLEDGEMENTS

Support for this research was provided by the National Science Foundation and The Goizueta Foundation.

REFERENCES

Alvarellos, J. 2003. *Fundamental Studies of Capillary Forces in Porous Media*, PhD Thesis, Georgia Institute of Technology, 188 pages.

Cascante, G. and Santamarina, J.C. 1996. Interparticle Contact Behavior and Wave Propagation, *ASCE Geotechnical Journal*, 122: 831-839.

Santamarina, J.C. and Cho, G.C. 2004. Soil Behavior: The Role of Particle Shape. *Proc. Skempton Conference*, March, London.

Díaz-Rodríguez, J.A. and Santamarina, J.C. 1999. "Thixotropy: The Case of Mexico City Soils", *XI Panamerican Conf. on Soil Mech. and Geotech. Eng*., Iguazu Falls, Brazil, 1: 441-448.

Dieterich, J. H. 1978. Time-dependent friction and the mechanics of stick-slip. *Pure Appl. Geophys*., 116: 790-806.

Fiegel, G.L., and Kutter, B.L. 1994. "Liquefaction mechanism for layered soils." *J. Geotech. Eng*., 120: 737-755.

Guimaraes, M. 2002. *Crushed stone fines and ion removal from clays.* PhD Thesis, Georgia Institute of Technology, 238 pages.

Kokusho, T. 1999. "Water film in liquefied sand and its effect on lateral spread." *J. Geotech. Geoenviron. Eng*., 125: 817-826.

Kuhn, M. R. and Mitchell, J.K. 1993. New Perspectives on Soil Creep, *ASCE J. Geotechnical Engineering*, 119: 507-524.

Kulhawy, F.H. and Mayne, P.W. 1990. *Manual on Estimating Soil Properties for Foundation Design*, Electric power Research Institute, Palo Alto.

Ladd, C.C., Foott, R., Ishihara, K., Schlosser, F. and Poulos, H.G. 1977. Stress-Deformation and Strength, *Proc. 9th ICSMFE*, 2: 421-494.

Landman, U., Luedtke, W.D. and Gao, J.P. 1996. Atomic-Scale Issues in Tribology: Interfacial Junctions and Nano-Elastohydrodynamics. *Langmuir*, 12: 4514-4528.

Leroueil, S. and Hight, D.W. 2003. Behaviour and properties of natural soils and soft rocks. In T.S. Tan, K.K. Phoon, D.W. Hight and S. Leroueil (eds), *Characterization and engineering Peoperties of natural Soils*: 29-254. Rotterdam: Balkema.

Mavko, G. M., Mukerji, T. and Dvorkin, J. 1998. *The Rock Physics Handbook*, New York: Cambridge University Press.

Mayne, P.W. and Holtz, R.D. 1985. Effect of principal stress rotation on clay strength, *Proc. 11th ICSMFE*, San Francisco, 2: 579-582.

Mitchell, J.K. 1960. Fundamentals aspects of thixotropy in soils. *Journal of the Soil Mechanics and Foundations Division*, ASCE, 86: 19-52.

Palomino, A. 2003. *Fabric formation and control in fine grained materials*, PhD Thesis, Georgia Institute of Technology, 193 pages.

Persson, N. J. 1998. *Sliding Friction. Physical Principles and Applications.* NanoScience and Technology, Springer-Verlag.

Randolph, M. 2002, Personal communication

Rothenburg, L. 1992) Effects of Particle Shape and Creep in Contacts on Micromechanical Behavior of Simulated Sintered Granular Media. ASME, *Mechanics of Granular Materials and Powder Systems*, MD 37: 133-142.

Santamarina, J.C., Klein, K. and Fam, M. 2001. *Soils and Waves*, Chichester: John Wiley & Sons.

Tatsuoka, F., Di Benedetto, H. and Nishi, T. 2003. A Framework for Modelling of the time effect on the stress-strain behaviour of geomaterials, In Di Benedetto et al. (eds), *Deformation Characteristics of Geomaterials*: 1135-1143. Lisse: Balkema.

Terzaghi, K., Peck, R. B. and Mesri, G. 1996. *Soil Mechanics in Engineering Practice*, New York: John Wiley & Sons.

Valdes, J.R. 2002. *Fines migration and formation damage - Microscale studies.* PhD Thesis, Georgia Institute of Technology, 241 pages.

Van Olphen, H. 1951) Rheological Phenomena of Clay Sols in Connection with the Large Distribution of Micelles, *Discussions of the Faraday Society*, 11: 82-84. (additional information in his book).

Velde, B. 1992. *Introduction to Clay Minerals: Chemistry, Origins, Uses and Environmental Significance*, New York: Chapman & Hall.

Vucetic, M. and Dobry, R. 1991. Effect of soil plasticity on cyclic response, *Journal of Geotechnical Engineering*, ASCE, 117: 89-107.

Wang, L., Fritton, S.P., Weinbaum, S, and Cowin, S.C. 2003. On bone adaptation due to venous stasis. *Journal of Biomechanics*, 36: 1439–1451.

Yoshimine, M., Robertson, P.K. and Wride, C.E. 1999. Undrained Shear Strength of Clean Sands to Trigger Flow Liquefaction, *Canadian Geotechnical Journal*, 36: 891-906.

Youd, T. L. 1973. "Factors controlling the maximum and minimum densities of sands", *Evaluation of Relative Density and its Role in Geotechnical Projects Involving Cohesionless Soils*, ASTM, Edited by Selig and Ladd, STP 523: 98-112.

Zdravkovic, L. and Jardine, R.J. 1997. Some Anisotropic Stiffness Characteristics of a Silt Under General Stress Conditions, *Géotechnique*, 47: 407-437.